

# Orientation-dependent strong-field dissociative single ionization of CO

QIYING SONG,<sup>1</sup> ZHICHAO LI,<sup>2</sup> HUI LI,<sup>1</sup> PEIFEN LU,<sup>1</sup> XIAOCHUN GONG,<sup>1</sup>  
QINYING JI,<sup>1</sup> KANG LIN,<sup>1</sup> WENBIN ZHANG,<sup>1</sup> JUNYANG MA,<sup>1</sup> HEPING ZENG,<sup>1</sup>  
FENG HE,<sup>2,3</sup> AND JIAN WU<sup>1,4</sup>

<sup>1</sup>State Key Laboratory of Precision Spectroscopy, East China Normal University, Shanghai 200062, China

<sup>2</sup>Key Laboratory of laser Plasmas (Ministry of Education) and Department of Physics and Astronomy, Collaborative innovation center for IFSA (CICIFSA), Shanghai Jiao Tong University, Shanghai 200240, China

<sup>3</sup>fhe@sjtu.edu.cn

<sup>4</sup>jwu@phy.ecnu.edu.cn

**Abstract:** The dissociative ionization of CO in orthogonally polarized femtosecond laser pulses are studied in a pump-probe scheme. The ionization of CO by the pump pulse and the dissociation of the created CO<sup>+</sup> by the probe pulse can be fully disentangled by identifying the photoelectron momentum distributions. Different from the dissociative ionization by a single pulse in which the CO molecule mostly breaks along the field polarization, in this pump-probe strategy, the CO<sup>+</sup> ion created from ionization by the pump pulse is favored to dissociate when it orients orthogonal to the polarization direction of the probe pulse. It is attributed to the laser-coupling of various electronic states of the molecular ion in the dissociation process, supported by the numerical simulation of a modeled time-dependent Schrödinger equation.

© 2017 Optical Society of America

**OCIS codes:** (020.2649) Strong field laser physics; (020.4180) Multiphoton processes; (260.3230) Ionization.

## References and links

1. P. Dietrich, D. T. Strickland, M. Laberge, and P. B. Corkum, "Molecular reorientation during dissociative multiphoton ionization," *Phys. Rev. A* **47**(3), 2305–2311 (1993).
2. C. Ellert and P. B. Corkum, "Disentangling molecular alignment and enhanced ionization in intense laser fields," *Phys. Rev. A* **59**(5), R3170–R3173 (1999).
3. A. S. Alnaser, C. M. Maharjan, X. M. Tong, B. Ulrich, P. Ranitovic, B. Shan, Z. Chang, C. D. Lin, C. L. Coker, and I. V. Litvinyuk, "Effects of orbital symmetries in dissociative ionization of molecules by few-cycle laser pulses," *Phys. Rev. A* **71**(3), 031403 (2005).
4. B. K. McFarland, J. P. Farrell, P. H. Bucksbaum, and M. Gühr, "High harmonic generation from multiple orbitals in N<sub>2</sub>," *Science* **322**(5905), 1232–1235 (2008).
5. I. Znakovskaya, P. von den Hoff, S. Zherebtsov, A. Wirth, O. Herrwerth, M. J. J. Vrakking, R. de Vivie-Riedle, and M. F. Kling, "Attosecond control of electron dynamics in carbon monoxide," *Phys. Rev. Lett.* **103**(10), 103002 (2009).
6. P. von den Hoff, I. Znakovskaya, S. Zherebtsov, M. F. Kling, and R. de Vivie-Riedle, "Effects of multi orbital contributions in the angular-dependent ionization of molecules in intense few-cycle laser pulses," *Appl. Phys. B* **98**(8), 659–666 (2010).
7. Q. Song, Z. Li, S. Cui, P. Lu, X. Gong, Q. Ji, K. Lin, W. Zhang, J. Ma, H. Pan, J. Ding, M. F. Kling, H. Zeng, F. He, and J. Wu, "Disentangling the role of laser coupling in directional breaking of molecules," *Phys. Rev. A* **94**(5), 053419 (2016).
8. J. Muth-Böhm, A. Becker, and F. H. M. Faisal, "Suppressed molecular ionization for a class of diatomics in intense femtosecond laser fields," *Phys. Rev. Lett.* **85**(11), 2280–2283 (2000).
9. X. M. Tong, Z. X. Zhao, and C. D. Lin, "Theory of molecular tunneling ionization," *Phys. Rev. A* **66**(3), 033402 (2002).
10. O. I. Tolstikhin, T. Morishita, and L. B. Madsen, "Theory of tunneling ionization of molecules: Weak-field asymptotics including dipole effects," *Phys. Rev. A* **84**(5), 053423 (2011).
11. N. Takemoto and A. Becker, "Multiple ionization bursts in laser-driven hydrogen molecular ion," *Phys. Rev. Lett.* **105**(20), 203004 (2010).
12. M. Abu-samha and L. B. Madsen, "Single-active-electron potentials for molecules in intense laser fields," *Phys. Rev. A* **81**(3), 033416 (2010).

13. A. S. Kornev and B. A. Zon, "Anti-Stokes-enhanced tunnelling ionization of polar molecules," *Laser Phys.* **24**(11), 115302 (2014).
14. A. S. Kornev, I. M. Semiletov, and B. A. Zon, "The influence of a permanent dipole moment on the tunneling ionization of a CO molecule," *Laser Phys.* **26**(5), 055302 (2016).
15. O. Smirnova, Y. Mairesse, S. Patchkovskii, N. Dudovich, D. Villeneuve, P. Corkum, and M. Yu. Ivanov, "High harmonic interferometry of multi-electron dynamics in molecules," *Nature* **460**(7258), 972–977 (2009).
16. J. Wu, M. Meckel, L. Ph. H. Schmidt, M. Kunitski, S. Voss, H. Sann, H. Kim, T. Jahnke, A. Czasch, and R. Dörner, "Probing the tunnelling site of electrons in strong field enhanced ionization of molecules," *Nat. Commun.* **3**, 1113 (2012).
17. A. S. Alnaser, S. Voss, X.-M. Tong, C. M. Maharjan, P. Ranitovic, B. Ulrich, T. Osipov, B. Shan, Z. Chang, and C. L. Cocke, "Effects of molecular structure on ion disintegration patterns in ionization of O<sub>2</sub> and N<sub>2</sub> by short laser pulses," *Phys. Rev. Lett.* **93**(11), 113003 (2004).
18. M. F. Kling, Ch. Siedschlag, A. J. Verhoef, J. I. Khan, M. Schultze, T. Uphues, Y. Ni, M. Uiberacker, M. Drescher, F. Krausz, and M. J. J. Vrakking, "Control of electron localization in molecular dissociation," *Science* **312**(5771), 246–248 (2006).
19. I. Znakovskaya, P. von den Hoff, S. Zherebtsov, A. Wirth, O. Herrwerth, M. J. J. Vrakking, R. de Vivie-Riedle, and M. F. Kling, "Attosecond Control of Electron Dynamics in Carbon Monoxide," *Phys. Rev. Lett.* **103**(10), 103002 (2009).
20. W. Lai and C. Guo, "Selective charge asymmetric distribution in heteronuclear diatomic molecules in strong laser fields," *Phys. Rev. A* **92**(1), 013402 (2015).
21. W. Zhang, Z. Li, P. Lu, X. Gong, Q. Song, Q. Ji, K. Lin, J. Ma, F. He, H. Zeng, and J. Wu, "Photon energy deposition in strong-field single ionization of multielectron molecules," *Phys. Rev. Lett.* **117**(10), 103002 (2016).
22. X. Sun, M. Li, Y. Shao, M. M. Liu, X. Xie, Y. Deng, C. Wu, Q. Gong, and Y. Liu, "Vibrationally resolved electron-nuclear energy sharing in above-threshold multiphoton dissociation of CO," *Phys. Rev. A* **94**(1), 013425 (2016).
23. R. Dörner, V. Mergel, O. Jagutzki, L. Spielberger, J. Ullrich, R. Moshhammer, and H. Schmidt-Böcking, "Cold target recoil ion momentum spectroscopy: a 'momentum microscope' to view atomic collision dynamics," *Phys. Rep.* **330**(98), 95–192 (2000).
24. J. Ullrich, R. Moshhammer, A. Dorn, R. Dörner, L. Ph. H. Schmidt, and H. Schmidt-Böcking, "Recoil-ion and electron momentum spectroscopy: reaction-microscopes," *Rep. Prog. Phys.* **66**(9), 1463–1545 (2003).
25. S. De, I. Znakovskaya, D. Ray, F. Anis, N. G. Johnson, I. A. Bocharova, M. Magrakvelidze, B. D. Esry, C. L. Cocke, I. V. Litvinyuk, and M. F. Kling, "Field-free orientation of CO molecules by femtosecond two-color laser fields," *Phys. Rev. Lett.* **103**(15), 153002 (2009).
26. S. De, M. Magrakvelidze, I. A. Bocharova, D. Ray, W. Cao, I. Znakovskaya, H. Li, Z. Wang, G. Laurent, U. Thumm, M. F. Kling, I. V. Litvinyuk, I. Ben-Itzhak, and C. L. Cocke, "Following dynamic nuclear wave packets in N<sub>2</sub>, O<sub>2</sub>, and CO with few-cycle infrared pulses," *Phys. Rev. A* **84**(4), 043410 (2011).

## 1. Introduction

When exposed to a strong laser field, molecules may break via the dissociative ionization which generally involves the ionization and dissociation processes depending on the molecular orientations with respect to the light polarization [1–7]. For the single ionization of a molecule, as described by the strong-field approximation [8] or molecular orbital Ammosov-Delone-Krainov theories [9,10], and numerically simulated by solving the time-dependent Schrödinger equation [11,12], electrons are favored to be freed by the laser field pointing along the maximal density distributions of the ionizing orbital, i.e. selective ionization of molecule with a given spatial orientation correlated to the orbital profile [13,14]. Although most of the models are based on the single-active-electron approximation by assuming tunneling ionization from the highest occupied molecular orbital (HOMO) [12], for a molecule with multiple electrons, e.g. electrons located in the next lower-lying orbitals, also participate in the strong field single ionization [4–6,15]. Furthermore, the electron localization assisted enhanced ionization [16] was identified to dominate the directional multiple ionization processes, in particular for multicycle laser fields in which the molecule could be stretched to the critical range of internuclear distance for multiple ionization.

Following the ionization, molecules may dissociate via laser coupling of various electronic states. By assuming the dominant molecular orientation selectivity of the ionization process, the emission direction of the ejected fragment ions of the dissociated molecule has been used to reconstruct the profile of the ionizing orbitals [3,17]. However, as compared to the ionization process, the dissociation itself assisted by the laser coupling also exhibits

dependencies on the spatial orientation of the molecular axis. Take the dissociative single ionization of  $H_2$  [18] as an example, the photon-coupled dipole transitions between the bound and dissociating states dominate the observed emission directions of the  $H^+$ , i.e.  $H_2$  is preferred to be broken along the field direction at the instant of photon coupling even the ionization process around the short equilibrium internuclear distance weakly depends on the molecular orientation. The knowledge of the orientation dependence of the dissociation process will certainly improve our understanding of the complicated dynamics of molecular dissociative ionization in strong laser fields.

CO has been chosen as a prototype system for heteronuclear molecules of which the dynamics have been widely studied when interacting with strong laser fields [19–22]. It is known that the detailed electronic structures of molecules play decisive role in the strong-field-molecule interactions. In this paper, we experimentally investigate the strong-field dissociative ionization of a multielectron system, i.e. CO, by identifying the ionization and dissociation processes based on the electron-ion coincidence measurement in a pump-probe scheme. Interestingly, by picking the ionization events triggered only by the pump pulse, we find that the dissociation of the  $CO^+$  by the time-delayed probe pulse is favored for the molecular ions orienting orthogonal to the polarization of the probe pulses. Our results indicate the essential role of molecular orientation in the laser-coupling assisted dissociation process when multielectron molecules exposed to intense femtosecond laser pulses.

## 2. Experimental setup

The experiments are performed in an ultrahigh vacuum reaction microscope of cold-target recoil ion momentum spectroscopy [23,24], which allows us to measure the three-dimensional momenta of the emitted electrons and ions from a single molecule in coincidence. A beam of femtosecond laser pulse (25 fs, 795 nm, 10 kHz) from a multipass Ti:sapphire amplifier is split into pump and probe arms by a beam splitter. The near-infrared (NIR) pump pulse is reflected to a dichroic mirror by a series of high reflective mirrors. The probe pulse is frequency doubled to generate the second-harmonic (SH) component in a 200- $\mu\text{m}$ -thick  $\beta$ -barium borate (BBO) crystal via the type-I phase matching. A motorized stage is employed in the probe arm to precisely control the time delay. The NIR pump pulse and the ultraviolet (UV) probe pulse are collinearly combined using a dichroic mirror. The co-propagating beam travels along the  $x$  axis and is afterwards sent into the vacuum chamber and be focused onto the molecular beam (propagates along the  $y$  axis) using a concave silver mirror with a focusing length of  $f = 75$  mm. The supersonic gas jet is generated by co-expanding a mixture of 10% CO and 90% He through a 30  $\mu\text{m}$  nozzle with a driving pressure of 1.5 bar. The intensities of the  $z$ -polarized pump pulse and the  $y$ -polarized probe pulse in the interaction region are estimated to be  $1.3 \times 10^{14}$  and  $8 \times 10^{13}$   $\text{W}/\text{cm}^2$ , respectively.

We investigate the dissociative single ionization of CO, i.e.  $CO + qh\nu \rightarrow C^+ + O + e$ , labeled as the CO(1, 0) channel. The whole processes can take place within one pulse (e.g. the pump pulse), or the CO ionized by the pump pulse ( $CO + nh\nu_{\text{pump}} \rightarrow CO^+ + e$ ) can be subsequently dissociated by the probe pulse ( $CO^+ + mh\nu_{\text{probe}} \rightarrow C^+ + O$ ). The latter case allows us to disentangle the ionization and dissociation processes by coincidentally detecting the ejected electrons and ions generated in the ionization and dissociation steps, respectively. To avoid the influence of the impulsive molecular alignment (rotational period  $T = 8.64$  ps for CO) excited by the pump pulse [25], the probe pulse is delayed by about 11 ps with respect to the pump pulse. In fact, we note that any time delays out of the revival time windows of the impulsive alignment induced by the pump pulse could work. In our measurement, the count rate on the electron detector is around 0.24 electrons per laser shot with an ion-to-electron count ratio of 0.4:1. The false coincidence is estimated to be  $\sim 10\%$ . To further suppress the electron-ion false coincidence, only the events with just one detecting electron are selected for the data analysis. In the following, we will first study the dissociative single ionization of CO

by a single beam of the pump or the probe pulses, and then disentangle the dissociation and ionization processes by the pump-probe scheme.

### 3. Experimental results

Figures 1(a) and 1(b) present the momentum distributions of  $C^+$  from the CO(1, 0) channel obtained from only one beam of pump or probe pulses. Both figures show more  $C^+$  events along the polarization directions of the driving fields (denoted by the red and blue arrows, respectively). This indicates that CO is preferred to be dissociative singly ionized when the molecular orientation is parallel to the field polarization direction. The corresponding kinetic energy release (KER) spectra of the nuclei are displayed in Fig. 1(c). Note that the kinetic energy of the non-detected neutral fragment O is calculated based on the momentum conservation of the breakup channel and is included in the KER of the CO(1, 0) channel. Discrete KER peaks spaced by  $\sim 0.17$  eV between 0 and 1.2 eV are observed for the CO(1, 0) channel by the NIR pump pulse [26], which comes from the vibrational structures of  $CO^+$  in  $A^2\Pi$  or  $B^2\Sigma^+$  states [see Fig. 1(d) for the potential curves of  $CO^+$ ].

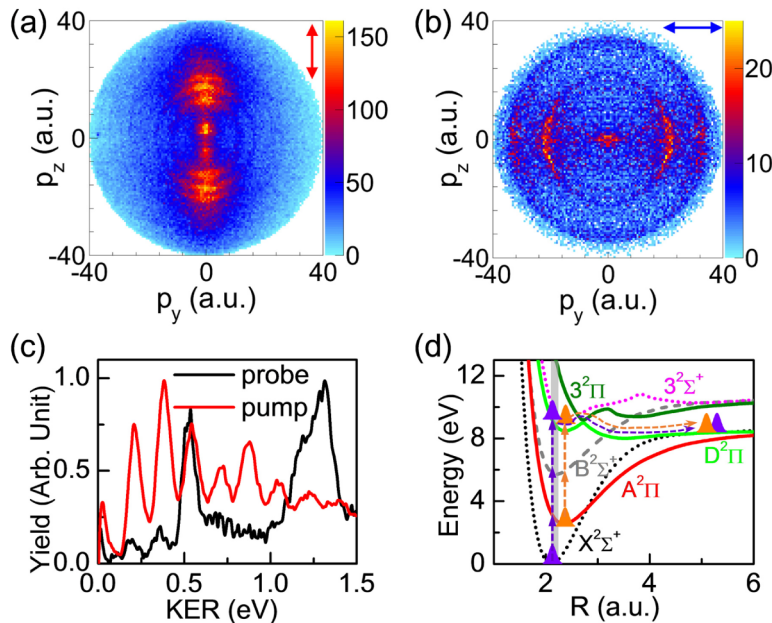


Fig. 1. Momentum distributions of  $C^+$  of CO(1, 0) channel dissociative ionized by the unique (a) 800 nm pump pulse (red arrow denotes the polarization of the driving field) and (b) 400 nm probe pulse (blue arrow denotes the polarization direction). (c) The KER spectra of CO(1, 0) channel for the pump (red solid curve) and probe (black solid curve) pulses, respectively. (d) The potential energy curves of the involved electronic states of  $CO^+$  (calculation method is described in [7,21]), where the gray bar indicates the Franck-Condon ionization region of the ground state CO. The violet and orange arrows illustrate the transition pathways for the dissociation of  $CO^+$  with molecular axis perpendicular and parallel to the UV field, respectively.

As compared to the results from the NIR pump pulses, the KER of the CO(1, 0) channel produced by a single beam of UV probe pulse can be distinguished in two regions, i.e.  $E_L$  region with KER  $< 0.7$  eV and  $E_H$  region with KER  $> 1.0$  eV. As displayed in Fig. 1(b), the angular distributions of the  $C^+$  for the  $E_H$  region (the outer ring) is broader than that for the  $E_L$  region. It is because that the  $E_L$  and  $E_H$  regions are produced via different pathways [21,22]. The  $E_H$  region is produced by removing one electron from HOMO-1 in the Frank-Condon region of CO, which populates the  $A^2\Pi$  state of  $CO^+$  and afterwards dissociates into  $C^+$  and O via the  $D^2\Pi$  state by absorbing two UV photons. On the other hand, the  $E_L$  region is produced

by removing a HOMO-2 electron at a large internuclear distance of stretched CO on the  $A^1\Pi$  state, which populates on the  $B^2\Sigma^+$  state and afterwards dissociates via the  $3^2\Pi$  or  $3^2\Sigma^+$  states.

Due to the entanglement of the ionization and dissociation steps, the orientation dependence of the dissociation process is hard to be distinguished in the measured angular distributions of the ionic fragments from dissociative ionization by a single laser pulse. We overcome this difficulty by exploiting an electron-ion coincidence measurement in a pump-probe scheme [7]. The neutral CO molecule is singly ionized by the pump pulse and the created randomly orientated molecular ion  $\text{CO}^+$  is afterwards dissociated by the time-delayed probe pulse. The electron-ion coincidence measurement allows us to pick out the right events. In detail, for the orthogonally polarized pump-probe laser pulses of different central wavelengths and field intensities in our experiments, electrons released by the pump and the probe pulses will show different angular distributions, which allows us to distinguish different processes. As shown in Fig. 2(a), the electron freed by the pump pulse is mainly concentrated within the white dashed ellipse along  $z$  axis (denoted as  $e_{\text{pump}}$ ), while the electron in the red dashed sectors along  $y$ -axis (denoted as  $e_{\text{probe}}$ ) is mainly freed by the probe pulse. Since only events with just one detected electron are selected, the observed  $\text{CO}(1, 0)$  channel correlated to electrons in the  $e_{\text{probe}}$  region stands for events that both ionization and dissociation are induced by the probe pulse. On the other hand, electrons in the  $e_{\text{pump}}$  region correspond to the events of which ionization is induced by the pump pulse, while the created  $\text{CO}^+$  could be dissociated into the  $\text{CO}(1, 0)$  channel either by the pump pulse itself or by the time-delayed probe pulse.

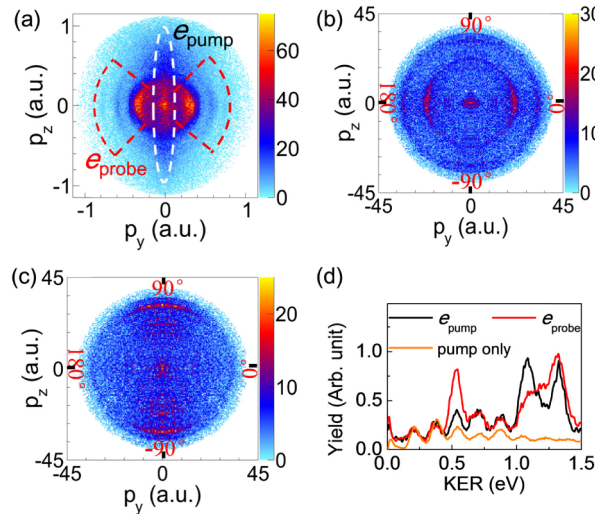


Fig. 2. (a) The momentum distribution of electrons for  $\text{CO}(1, 0)$  channel in the pump-probe experiment. Electrons distributed in white dashed ellipse ( $e_{\text{pump}}$ ) and red dashed sectors ( $e_{\text{probe}}$ ) are released by the pump pulse and the probe pulse, respectively. The momentum distribution of  $\text{C}^+$  ions for  $\text{CO}(1, 0)$  channel measured in coincidence with electrons in (b)  $e_{\text{probe}}$  and (c)  $e_{\text{pump}}$ . (d) KER spectra of  $\text{CO}(1, 0)$  channel correlated to the momentum distributions in (b) and (c) and KER spectrum of  $\text{CO}(1, 0)$  channel contributed by a single pump beam.

To extract the pump-ionization probe-dissociation events for the  $\text{CO}(1, 0)$  channel, we analyzed the momentum distributions and KER spectra measured in coincidence with the electrons in the  $e_{\text{probe}}$  and  $e_{\text{pump}}$  regions. The  $\text{C}^+$  fragment ions correlated to electrons in different regions exhibit different momentum distributions, as displayed in Figs. 2(b) and 2(c). In Fig. 2(b), associated with the electrons in  $e_{\text{probe}}$  region, the  $\text{C}^+$  mainly emits along the polarization direction of the probe pulse, i.e. along  $\phi_{\text{C}^+} = 0^\circ$  or  $180^\circ$ . The corresponding KER distribution is plotted in Fig. 2(d) (red solid curve). Both the momentum distributions and the

KER spectra are similar to the results obtained by a single probe pulse. The features induced by the pump pulse are also encoded in the spectrum, represented by the KER peaks with  $\sim 0.17$  eV interval. Interestingly, as displayed in Fig. 2(c), the momentum distribution of the  $C^+$  ions associated with the electrons in the  $e_{\text{pump}}$  region (pump-ionization and probe-dissociation) dominate along  $\phi_{C^+} = \pm 90^\circ$ , which is perpendicular to the polarization direction of the probe pulse. The corresponding KER spectrum is plotted in Fig. 2(d) (black solid curve). Comparing to the results obtained from a single beam of pump pulses [Fig. 1(a) and the orange curve in Fig. 2(d)], the significant differences can be attributed to the events involving pump-ionization and probe-dissociation processes. Noticeable signals with the KER peaked at 1.1 eV and 1.3 eV are observed which are from the dissociation of the orthogonally aligned molecular ions by the probe pulse. This enhancement in the  $C^+$  ion yield for  $KER > 0.9$  eV can only be obtained when an electron in the neutral molecule is freed by the pump pulse and gets a final momentum in the  $e_{\text{pump}}$  region [shown in Fig. 2(a)]. Besides, the spectrum in the region of 0 to 0.9 eV is comparable to the one obtained from a single pump pulse, implying that this part is mainly induced by the pump pulses.

#### 4. Numerical simulations and discussions

In order to understand the pump-ionization probe-dissociation process, we firstly calculated the ionization probabilities to different electronic states of  $CO^+$  by the strong-field approximation [8]. According to our calculations, the initial population ratio in the  $X^2\Sigma^+$  and  $A^2\Pi$  states of  $CO^+$  is about 100:1. The ionization probability of removing one electron from HOMO ( $\sigma$  symmetry) of CO is maximal when the molecular axis is parallel to the laser field, while removing one electron from HOMO-1 ( $\pi$  symmetry) of CO the ionization probability is maximal when the molecule axis perpendicular to the polarization of the laser field [13,14]. For the dissociation process, we numerically solved the time dependent Schrödinger equation (for details of the model please see Ref [7].). We put the ground state of CO on the  $X^2\Sigma^+$  and  $A^2\Pi$  states with a ratio of 100:1 and simulate the dissociation dynamics for an ensemble of randomly oriented molecular ions in a UV laser field polarized along  $y$  axis. The calculated momentum distributions and the KER spectrum are plotted in Fig. 3. In comparison with the experimental results shown in Figs. 2 (c) and 2(d), the enhanced two spectral peaks above 1 eV [corresponding to the signal rings at radial momenta of about 30 a.u. in Fig. 3(a)] are obtained. A qualitative agreement is reached here. In the simulations, the coupling between the  $X^2\Sigma^+$  and  $A^2\Pi$  states of  $CO^+$  by the UV probe pulse is included. As illustrated by violet arrows in Fig. 1(d), initialized from the  $X^2\Sigma^+$  state of  $CO^+$ , the nuclear wave packets climb a ladder through  $X^2\Sigma^+ - A^2\Pi - B^2\Sigma^+ - D^2\Pi$  states by absorbing one- $\omega_{\text{SH}}$ -photon in each step and dissociates into  $C^+$  and O fragments.

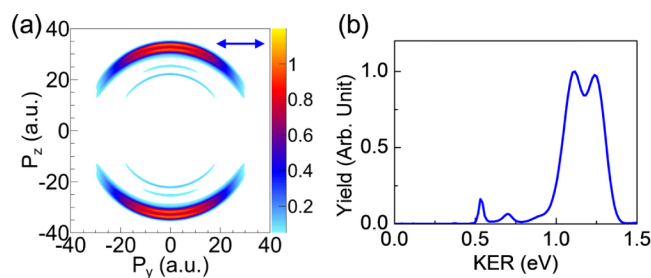


Fig. 3. The calculated (a) momentum distribution and (b) KER spectrum of  $C^+$  for the  $CO(1, 0)$  channel. The blue arrow in (a) denotes the polarization of the driving field.

Based on the transition selection rules, the laser field perpendicular to the molecular axis triggers the transition between  $^2\Sigma^+$  and  $^2\Pi$ , while the field parallel to the molecular axis induces the transition between all  $^2\Pi$  states. The energy difference between the  $^2\Sigma^+$  and  $^2\Pi$  states is about one photon energy of the SH near the Franck-Condon region. The nuclear

wave packets can climb a ladder through  $X^2\Sigma^+ - A^2\Pi - B^2\Sigma^+ - D^2\Pi$  states by absorbing one- $\omega_{SH}$ -photon in each step, i.e. the perpendicular transition as illustrated by violet arrows in Fig. 1(d). For the parallel transition, the nuclear wave packet propagating on the  $A^2\Pi$  state undergoes a two- $\omega_{SH}$ -photon transition to the  $D^2\Pi$  state, as illustrated by orange arrows in Fig. 1(d). Transitions involving two-photon absorption are intrinsically less probable than the single photon processes thus the ladder climbing process can result in a higher probability for the perpendicular transitions. This explains the preferred dissociation for the orthogonal orientated  $CO^+$ .

The simulation results reveal the importance of laser coupling of various electronic states for orientation dependent dissociation. The ionic molecular orientation is pre-selected by the ionization process before the dissociation, which reduces the visibility of laser coupling of electronic states on the eventually observed orientation dependence of the dissociative ionization by a single laser pulse. Utilizing the pump-ionization probe-dissociation scheme, we can disentangle the contributions of the orientation dependences in the ionization and dissociation steps for the dissociative single ionization of  $CO$ .

## 5. Conclusion

To summarize, taking  $CO$  as a prototype, by disentangling the coexisting ionization and dissociation processes, the orientation-dependent dissociation is observed, which clearly demonstrates the feasibility of the strategy of disentangling the ionization and dissociation steps. The qualitative agreement between quantum simulations and experimental results explores the importance of intermediate states in the dissociative ionization of multielectron molecules. Our technique by coincidentally distinguishing electrons and ions released by pump and probe pulses of various polarizations can be used to dig many interesting phenomena in ionization and dissociation of complex molecules, and further to steer the molecular reactions through selective pathways.

## Funding

National Natural Science Foundation of China (Grant Nos. 11425416, 61690224, 11621404, 11175120, 11574205, and 11322438).